CFD Letters 16, Issue 6 (2024) 120-130

CFD Letters

Journal homepage:
https://semarakilmu.com.my/journals/index.php/CFD_Letters/index
ISSN: 2180-1363

Modeling and Simulation of Elastohydrodynamic Lubrication in Spur Gears

Rafael Ramirez [1,*], Andrés Rodríguez[2], Jonathan Fábregas[2,3], Heriberto Maury[4]

[1] Mechanical Engineering Department, Universidad del Atlántico, Barranquilla, Colombia
[2] Universidad de la Costa, Energy Department, Cl. 58 #55-66, 080002, Barranquilla, Colombia
[3] Mechanical Engineering Department, Universidad Autónoma del Caribe, Barranquilla, Colombia
[4] Mechanical Engineering Department, Universidad del Norte, Barranquilla, Colombia

ARTICLE INFO

Article history:
Received 10 August 2023
Received in revised form 12 September 2023
Accepted 19 October 2023
Available online 21 January 2024

Keywords:
Elastohydrodynamic lubrication; Multiphysics; Simulations; Fluid dynamics; Thickness of lubricant film

ABSTRACT

An analysis using computational modeling by finite elements of the phenomenon of elastohydrodynamic lubrication (EHL) was carried out for a transmission system of pinion gear in a crankcase with partial filling lubrication. The analysis utilized tribological studies describing the contact behavior characteristics of solid surfaces with the lubrication film caused by dragging and splashing. Furthermore, the characteristics of the Reynolds-Hertz model for this type of phenomena are described, as well as the equations of elastic deformation and elastic displacements along with the geometry of the non-concordant bodies in contact. This was done by modeling the Lagrangian-Eulerian type for non-Newtonian fluid, implementing multiphysics coupling methods. The pressure profile of the lubricant films, the temperature reached by the lubricant, and the von Mises stress at the contact were obtained, showing a good approximation with the related results, indicating a range of 30 MPa to 900 MPa of pressure in the lubricant film and von Mises stress ranging from 30 MPa to 100 MPa in the contact area of the gear tooth.

1. Introduction

In a great variety of mechanisms such as gears, cam follower pairs, and bearings, their elements are coupled and interact through pairs in which the contact between the surfaces starts from a point or a line. The loads are transmitted between other bodies are confined to this area resulting in pressures and stress concentration, in turn, causing the tribological processes rigged to direct contact and the relative movement of surfaces such as wear and friction, which are responsible for the damage to components and the dissipation of energy, are quite severe. This is because lubrication is crucial for the good performance of this type of mechanism. The purpose of the application of a lubricant is to prevent direct contact by forming a film of sufficient thickness sandwiched between the two solid bodies to withstand the normal load transmitted by the contact and to adapt to the difference in tangential velocity between the two surfaces. Therefore, there is technological interest

* *Corresponding author.*
E-mail address: rafaelramirez@mail.uniatlantico.edu.co (Rafael Ramírez)

https://doi.org/10.37934/cfdl.16.6.120130

in calculating the thickness of the lubricating film and comparing it to the roughness of real surfaces to anticipate some potential contact between the surfaces and, in this way, to ensure a reliable design of these systems.

In the aforementioned mechanisms, where the high hydrodynamic pressures exerted by the lubricating film cause large elastic deformations of surfaces and changes in the lubricant's viscosity which in turn, affect the formation of the lubricating thickness film, the lubrication condition that takes place, receives the name of EHL.

This involves a coupling of different physical aspects including hydrodynamics, elasticity, thermodynamics, and heat transfer and as a result, a highly nonlinear problem that is particularly difficult to solve. In works such as those by Qin *et al.,* [1] it was found that the elastohydrodynamic rigidity contact is close to Hertzian contact rigidity in high loads cases, low speeds, and small bend radius; critical conditions in which the elastohydrodynamic rigidity can be approximated by the Hertzian rigidity, are investigated and verified by the valve dynamic simulation train in a diesel engine.

On the other hand, Peng *et al.,* [2] presented a novel model of EHL with the thermal focus for the non-Newtonian liquid used in helical gears with modifications and misalignments, used an asymmetric spherical roller for contact, between the modified toothed surfaces incorporating maladjustments, together with a load distribution model, investigating the effects of modifications and imbalances in the tribological behavior. In their results, they indicate the contact of the edge leads to high pressure and temperature, as well as a thin thickness film, showing a good behavior for the mismatch.

Habchi [3] in his study found that friction can be controlled in elastohydrodynamic contacts by an appropriate choice of surface coatings based on thermal properties. Low thermal inertia coatings would reduce friction, while high thermal inertia coatings would increase it. Guo *et al.,* [4] incorporated an algorithm that directly provides the elastic deformation in a finite line contact EHL lubrication analysis for a steel roller system in glass discs. Bair [5] uses the 1952 McEwen equation to accurately describe the pressure-viscosity effect at low pressures, highlighting the importance of the model for the film thickness classic formation EHL, obtaining parameters for several low viscosity liquids.

Tsuha *et al.,* [6] propose an approach for the representation of the contact boundary layer studies with EHL according to the rigidity parameters, applying it in a follower cam system, obtaining the evaluation of EHL for the different speeds. Nikas [7] analyzed analytically the effects of traction on the normal displacements for numerical tests in an elliptical contact with EHL comparing with known published formulas. Obtaining the percentages of errors for the effects of traction and show that the thickness of the central film is not affected by the simplification of the traction factor, but the minimum thickness of the film is significantly overestimated.

In Bujurke *et al.,* [8], Habchi [9], Paulson *et al.,* [10] and Stupkiewicz *et al.,* [11] finite element models were used to study the effects of fully coupled EHL for the thermomechanical solution, in their results they demonstrate the importance of the computational implementation for the solution of the rheological models the EHL implement, comparing it with the response times and conventional studies. In other related studies, contact friction is designed analytically in the involute of gears, as well as the simulation of non-newtonian liquids, CFD applications, DOE design of experiments, and remeshing in deformable systems by finite elements, as also indicated in Ref. [12-26].

Therefore, in the present research, the study of a transmission box with a pinion and a gear is carried out regarding the rheological and mechanical effects that affect the contact moment of the system, since these allow establishing the optimum parameters of operation and selection of materials with respect to a failure criterion. For this purpose, the modeling and simulation of a simple transmission system consisting of a pair of pinions with straight-toothed wheels with a splash and drag lubrication system are proposed using EHL modeling. In this system, the lubricant is stored in a reservoir or crankcase and one of the gears is partially immersed in it, which picks up the oil as it rotates, transports it, and splashes it to the contact points.

2. Materials and Method

A rheological or constitutive model of a fluid describes how it reacts and behaves in response to different physical inputs or actions. The main physical inputs to be taken into account when studying the behavior of a lubricant are mechanical actions (forces, pressures, stresses, and deformations) and thermal actions (temperature differences and heat flows) among others.

Properties such as dynamic viscosity η, shear stress τ, speed gradient $\dot{\gamma} = (\partial v/\partial n)$, the kinematic viscosity ν, the density of the lubricant ρ have a fundamental role in lubrication. In EHL the viscosity and density are extremely sensitive to changes in pressure and temperature.

The density of most mineral oils increases with pressure. Frequently this effect is small and can be neglected. However, at the great pressures that occur in elastohydrodynamic contacts, the lubricant cannot be considered as an incompressible medium. An empirical relation describing this dependence according to the formula proposed by Dowson and Higginson which incorporates the temperature dependence, is presented below:

$$\rho(p,\theta) = \rho_0 \frac{(C_1+C_2 p)}{(C_1+p)}\left[1-\lambda(\theta-\theta_0)\right] \tag{1}$$

where ρ_0 is the density at ambient conditions, λ is the thermal expansion coefficient, θ_0 is the ambient temperature and C_1 = 5.9 × 108 and C_2 = 1.34 are constants.

The relevant behaviors of a lubricant in the EHL condition are mainly the non-newtonian viscous rheological behavior, which relates in a non-linear way the stress measurements and the deformation rates. One way to approach this behavior is to combine the Ree-yring model, the visco-plastic model, the simplified visco-plastic model of Bair-Winer, and the circular visco-plastic model obtaining the following expression:

$$\sigma(\theta,p,d) = -pI - \frac{\tau_0\sqrt{2d{:}d}\left(\frac{2}{3}tr(d)d+2d\right)}{2d{:}d} * \operatorname{arcsinh}\left(\frac{\sqrt{2d{:}d}\,\eta_0 \exp^{\left\{[\ln(\eta_0)+9.67]\left[\left(1+\frac{p}{p_0}\right)^{Z}-1\right]\left[\frac{\theta-138}{\theta_0-138}\right]^{S_0}\right\}}}{\tau_0}\right) \tag{2}$$

Where p is the thermodynamic pressure, d is the Eulerian strain tensor, I is the spatial unitary tensor, η_0 is the generalized viscosity, τ_0 is the tensile strength by shear at p = 0, the constant p_0 = 1.98 × 108 Pa, θ is the absolute temperature of interest in the lubricant, Z and S0 are constant characteristics of the lubricant in particular, independent of temperature and pressure. These constants can be calculated from the following equations:

$$Z = \frac{\alpha p_0}{\ln(\eta_0)+9.76} \tag{3}$$

$$S0 = \frac{\beta(\theta_0-138)}{\ln(\eta_0)+9.76} \tag{4}$$

where α is the pressure-viscosity coefficient [m^2/N], for mineral oils α is generally in the range of 10-8 to 2 × 10-8.

2.1 Numerical Implementation

The computational implementation of the mathematical models formulated for EHL in a system of spur gears is presented in detail, using engineering simulation software with capacity for structural mechanics, fluid dynamics, heat transfer, and multiphysics simulations. The numerical methods with which simulation is approached are the finite element method, used mainly for structural mechanics, and the finite volume method, which is the numerical scheme in fluid dynamics.

It is carried out by means of execution of coupling the simultaneous solution of processes in an external tool configured in the software for the solution of one or several platforms named as coupling of systems, for this case APDL (structural) and CFD relating the interface conditions in the place where the teeth of the gears and the lubricant make contact. It became necessary to configure mesh reconstruction techniques due to the excessive deformation in the volumetric cells (elements) that appear when activating the rotation of the gears in the lubricating fluid domain, establishing as a priority the zones of interest and frontiers affected by the deformation.

The expressions used for the implementation of the mathematical models are represented below. Constant for the compressibility of the lubricant equation: C_1 = 0.6 × 10-9 kg^{-1} m s^2, C_2 = 1.7×10-9 kg^{-1} m s^2, C_3 = 0.65 × 10-3 K-1. The initial height of the lubricant in the crankcase:

$$S_0 = betaTV * \frac{T0-138[K]}{loge\left(\frac{visc0}{1\,[kg\,m^{-1}s^{-1}]}\right)+9.76} \tag{5}$$

where ambient temperature T0 = 313 K, the expression for the initial volume fraction of Air (VFA0) and the expression for the initial volume fraction of lubricant (VFL0), the constant for the viscosity Z0, the piezo-viscous coefficient alpha = 2.19 × 10-8 kg^{-1} m s^2, the thermal-viscous coefficient betaTV = 0.042 K^{-1}, the ambient pressure p0 = 1.98 × 108 kg m^{-1} s^{-2}, the lubricant compressibility density (rho), the initial density at initial conditions rho0 = 870 kg m^{-3}, eyring yield stress tao0 = 5 × 106 kg m^{-1} s^{-2}, viscosity to initial conditions visc0 = 0.075 kg m^{-1} s^{-1}.

$$VFA0 = step\left(\frac{y-H}{1[m]}\right) \tag{6}$$

$$VFL0 = 1 - VFA0 \tag{7}$$

$$Z0 = alpha * \frac{p0}{loge\left(\frac{visc0}{1\,[kg\,m^{-1}s^{-1}]}\right)+9.76} \tag{8}$$

$$rho = rho0 * \left(1 + C1 * \frac{pabs}{1+C2*pabs} - C3 * (T - T0)\right) \tag{9}$$

$$viscEyring = \left(\frac{tao0}{sstrnr+0.00001[s^{-1}]}\right) * ln\left(\left(viscHoupert * \frac{sstrnr}{tao0}\right) + sqrt\left(\left(viscHoupert * \frac{sstrnr}{tao0}\right)^2 + 1\right)\right) \tag{10}$$

$$viscHoupert = visc0 * exp\left(\left(loge\left(\frac{visc0}{1\,[kg\,m^{-1}s^{-1}]} + 9.67\right)\right) * \left(\left(1 + \frac{pabs}{p0}\right)^{Z0} - 1\right) * (fe)\right) \tag{11}$$

2.2 Boundary Conditions

The gearing of the gear system was designed using CAD tools and was done according to the involute system. The basic gear parameters that were modeled are:

The number of pinion teeth of 35, Number of gear teeth of 140, Modulus of 2 mm, Nominal pressure angle of 20°, Tooth width of 20 mm.

For the simulation system, two stages were carried out in which, the first stage comprises the splash and the drag of lubricant that was necessary in order to develop a distribution and an initial state of the lubricant in the contact zone before starting the transient EHL simulation properly. The interest in this stage of the process is the lubricant obtaining at the contact points. The second stage studies the formation of the elastohydrodynamic film between pairs of teeth involved in the transmission by a range of movement of the gear of approximately the arc of action. During this stage, all relevant factors for the EHL are considered such as elastic deformation of the transmission surfaces, non-newtonian rheology, and lubricant compressibility.

For the assembly and modeling of the system, the physical and mechanical properties of the materials shown below in Table 1 and Table 2 are used.

Table 1
Properties of steel used for gears

Specific heat [J/kg K]	Isotropic thermal conductivity [W/m K]	Burst limit load by traction [Pa]	Compression elasticity limit [Pa]	Density [kg/m^3]
434	60.5	4.6 e 08	2.5 e 08	7850

Table 2
Properties of the lubricant used

Dynamic viscosity	Thermal conductivity [W/mm k]	Specific Heat [J/kg k]	Density
viscEyring	1.4e-05	2000	rho

For the border conditions, pairs of the revolution were added in reference to the pinion and the gear in their internal cylindrical faces. An angular velocity load of 1000 rpm was added to the pinion revolution joint, and a 458 Nm resistive torque was imposed on the gear revolution joint. The process conditions are shown in Figure 1.

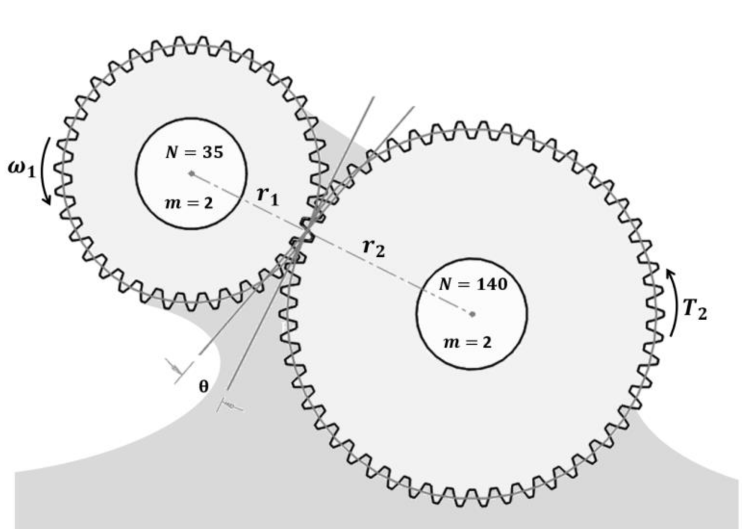

Fig. 1. Spur gear drive system

3. Results

Once the simulation runs have been carried out through the execution of couplings for multiphysics, mass continuity profiles, temperature distributions in the contact areas of interest, distribution of pressure and stress fields, and thickness of lubricant film in the contact area between pinion - gear are obtained. For the first stage of solution, the progression of the lubricant flow is obtained during the dragging and splashing of the same by the gear from the initial moment in which the lubricant rests at the bottom of the box (crankcase) to a flow in stable states, it is shown in Figure 2.

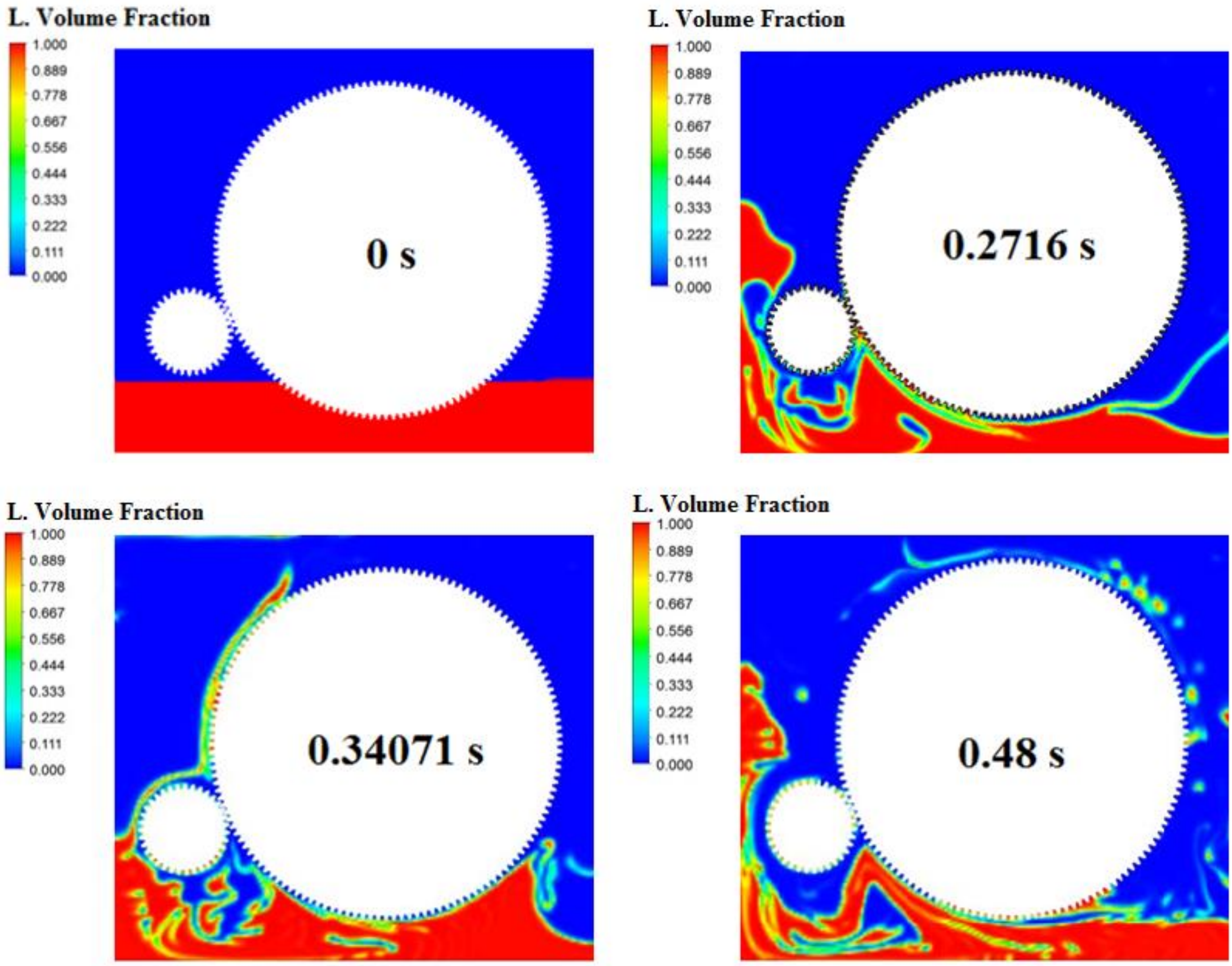

Fig. 2. Lubricant distribution in the transmission system

In Figure 2, the lubricant distributions at instants of consecutive time are represented by the volume fraction field. The red areas represent the pure lubricant, the blue ones indicate they are entirely occupied by air, and the intermediate colors represent mixtures in different proportions of the two phases.

The solution of the system was established until the moment when the oil flow covers the contact area of the gears completely. Figure 3 shows in detail the lubricant distribution around the gearwheels of the gear. It can be observed that the contact zone, formed by the three pairs of teeth in contact, is completely occupied by the lubricant.

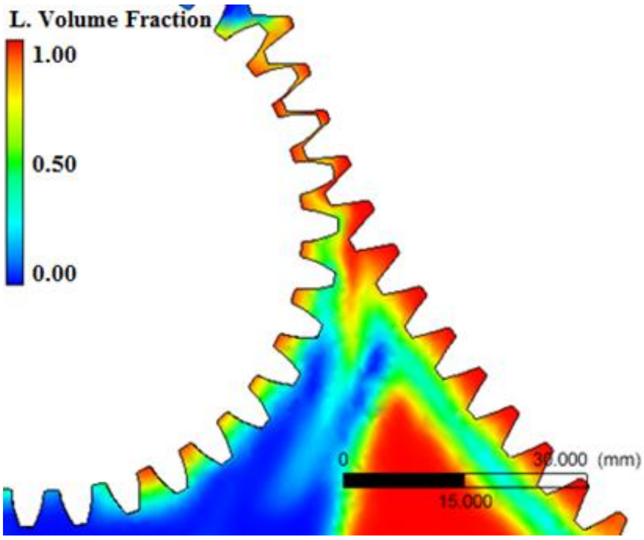

Fig. 3. Lubricant distribution in the arc of action of the transmission

The solution that provides the results of the second stage is obtained by the solution of the models in the first stage, for that reason in Figure 4, the distribution of the lubricant film thickness between a pair of intermeshed teeth is shown when the pressure reaches the maximum in the path that comprises the action arc of the gear.

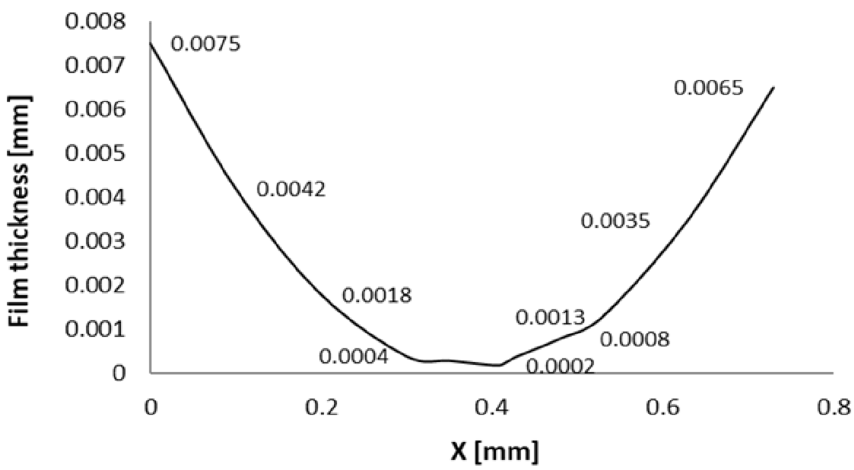

Fig. 4. Lubricant film thickness distribution in the action arc of the gear

As if it is shown in Figure 4, the minimum thickness of the film takes approximately a value of 0.0002 mm. this result can be compared with the previous studies where the thickness of the film was below 0.0025 mm, as also indicated in [27].

Figure 5 shows pressure and temperature in a consecutive instant of time where a couple of teeth are interacting during the arc of action of the gear. The distribution profiles of pressure versus the length measured along sectional curve of contact they regular values between 30 MPa and 900 MPa. They are approximately located to the half of the contact zone. This pressure profile can be explained by the elastic responses of the teeth by the strength made by the lubricant. The temperature profiles showed at the impact zone show a range that goes from 335 K to 480 K. Previous studies such as those by [27], show that the maximum pressures are understood in a range between 0.05 and 1.2 GPa.

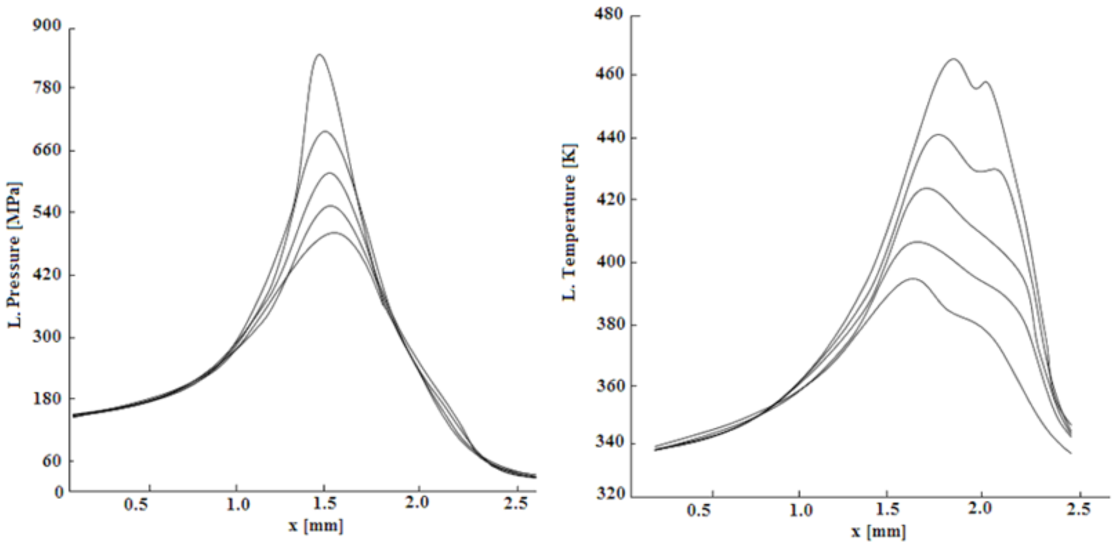

Fig. 5. Temperature and pressure profile in the contact zone

Figure 6 and Figure 7 are shown for illustrative and explanatory purposes. The profile of the equivalent Von Mises stresses and lubricant pressure at the instant of contact on the tooth transmission surfaces is shown in Figure 6.

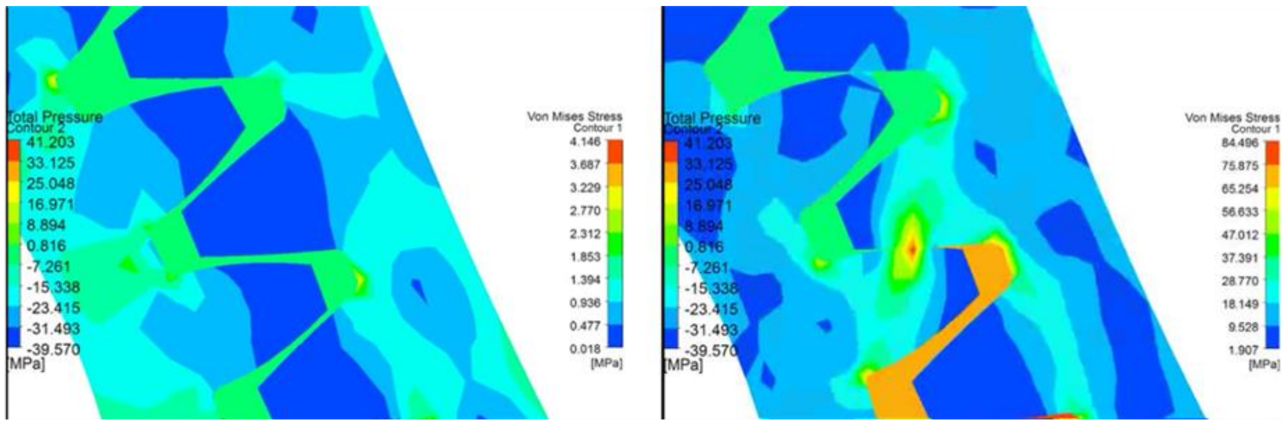

Fig. 6. Equivalent Von Mises stress profile on the transmission's surfaces

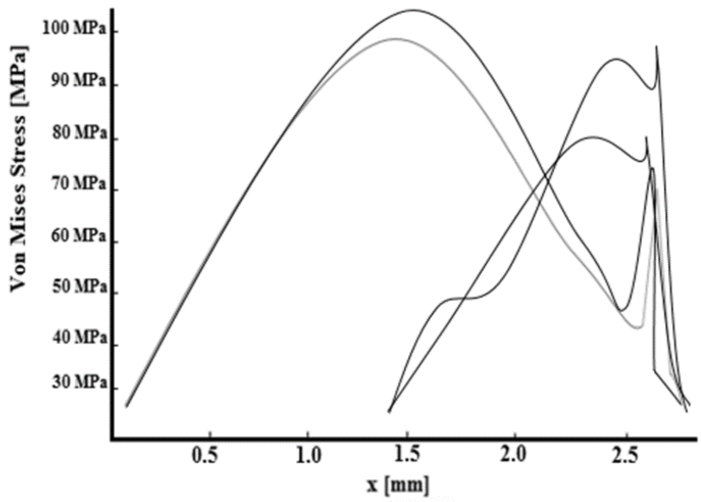

Fig. 7. Equivalent Von Mises stress at the transmission's surfaces

The curves corresponding to the stress are represented for Von Mises of one of the teeth of the pinion on having contacted the lubricated gear indicating values in the ranges of 30 MPa and 100 MPa, which are kept in the elastic zone for the material used. The curves at the right show the beginning of the contact while the curves at the center correspond to the average points of contact of the transmission. In similar research such as those of [9, 10, 28] the EHL was developed obtaining the characteristic curves of the contact stress presenting magnitudes and graphs of curves in accordance with the present study. On the other hand, experimentally studies of spur gears are used for the detection of mechanical failures [29].

4. Conclusions

In conclusion, the simulation and analysis of thermo-EHL in a system of spur gears were successfully conducted through the multiphysical coupling of CFD and structural mechanics tools. These tools provided insights into the mechanical, thermal, and fluid dynamic effects in the EHL process.

The programming of the simulated models to characterize the lubrication of the system was capable of encompassing a wide range of physical effects, including non-Newtonian fluid behavior, piezoviscosity, and thermoviscosity.

The low-time-step iterations performed by the solver in the post-processing stage of the simulation allowed for tracking the lubricant splash stage on the gear teeth. The lubricant film thickness obtained on the contact surfaces of the gears remained within the operational ranges indicated by the EHL literature.

The Von Mises stresses presented on the contacting gear teeth during the EHL process stayed within the elastic zone of the material's strength used in the study, meeting the objective of the EHL phenomenon.

Furthermore, the pressure reached by the lubricant film during the mechanical transmission contact falls within the ranges consistent with EHL research, where limits of up to 1.2 GPa of lubricant film pressure have been established.

Acknowledgement
This research was not funded by any grant.

References

[1] Qin, Wenjie, Jie Chao, and Lunjing Duan. "Study on stiffness of elastohydrodynamic line contact." *Mechanism and Machine Theory* 86 (2015): 36-47. https://doi.org/10.1016/j.mechmachtheory.2014.12.001

[2] Peng, Yanjun, Ning Zhao, Mengqi Zhang, Wang Li, and Ruchuan Zhou. "Non-Newtonian thermal elastohydrodynamic simulation of helical gears considering modification and misalignment." *Tribology International* 124 (2018): 46-60. https://doi.org/10.1016/j.triboint.2018.03.025

[3] Habchi, W. "Thermal analysis of friction in coated elastohydrodynamic circular contacts." *Tribology International* 93 (2016): 530-538. https://doi.org/10.1016/j.triboint.2015.01.017

[4] Guo, L., W. Wang, Z. M. Zhang, and P. L. Wong. "Study on the free edge effect on finite line contact elastohydrodynamic lubrication." *Tribology International* 116 (2017): 482-490. https://doi.org/10.1016/j.triboint.2017.08.010

[5] Bair, Scott. "Pressure–viscosity response in the inlet zone for quantitative elastohydrodynamics." *Tribology International* 97 (2016): 272-277. https://doi.org/10.1016/j.triboint.2016.01.037

[6] Tsuha, Natália Akemi Hoshikawa, Fábio Nonato, and Katia Lucchesi Cavalca. "Formulation of a reduced order model for the stiffness on elastohydrodynamic line contacts applied to cam-follower mechanism." *Mechanism and Machine Theory* 113 (2017): 22-39. https://doi.org/10.1016/j.mechmachtheory.2017.03.002

[7] Nikas, George K. "Miscalculation of film thickness, friction and contact efficiency by ignoring tangential tractions in elastohydrodynamic contacts." *Tribology International* 110 (2017): 252-263. https://doi.org/10.1016/j.triboint.2017.02.022

[8] Bujurke, N. M., M. H. Kantli, and Bharati M. Shettar. "Wavelet preconditioned Newton-Krylov method for elastohydrodynamic lubrication of line contact problems." *Applied Mathematical Modelling* 46 (2017): 285-298. https://doi.org/10.1016/j.apm.2017.01.074

[9] Habchi, Wassim. "A numerical model for the solution of thermal elastohydrodynamic lubrication in coated circular contacts." *Tribology International* 73 (2014): 57-68. https://doi.org/10.1016/j.triboint.2014.01.002

[10] Paulson, Neil R., Farshid Sadeghi, and Wassim Habchi. "A coupled finite element EHL and continuum damage mechanics model for rolling contact fatigue." *Tribology International* 107 (2017): 173-183. https://doi.org/10.1016/j.triboint.2016.11.024

[11] Stupkiewicz, Stanisław, Jakub Lengiewicz, Przemysław Sadowski, and Stanisław Kucharski. "Finite deformation effects in soft elastohydrodynamic lubrication problems." *Tribology International* 93 (2016): 511-522. https://doi.org/10.1016/j.triboint.2015.03.016

[12] Lai, Xiao. "The Finite Element Transient Structure Analysis of the Startup of the Sugarcane Harvester Transfer Case." *International Journal of Engineering* 29, no. 7 (2016): 968-974. https://doi.org/10.5829/idosi.ije.2016.29.07a.12

[13] Fabregas Villegas, J., Arnold Martínez Guarín, and Jimy Unfried-Silgado. "A coupled rigid-viscoplastic numerical modeling for evaluating effects of shoulder geometry on friction stir-welded aluminum alloys." *International Journal of Engineering* 32, no. 2 (2019): 313-321. https://doi.org/10.5829/ije.2019.32.02b.17

[14] Ismail, Mohamad Alif, Mohamad Hidayad Ahmad Kamal, Lim Yeou Jiann, Anati Ali, and Sharidan Shafie. "Transient Free Convection Mass Transfer of Second-grade Fluid Flow with Wall Transpiration." *CFD Letters* 13, no. 11 (2021): 35-52. https://doi.org/10.37934/cfdl.13.11.3552

[15] Ariffin, Noor Amalina Nisa, Iskandar Waini, Abdul Rahman Mohd Kasim, Mohamad Hidayad Ahmad Kamal, Mohd Rijal Alias, and Seripah Awang Kechil. "Numerical Solutions on Reiner–Philippoff (RP) Fluid Model with Velocity and Thermal Slip Boundary Condition." *CFD Letters* 14, no. 12 (2022): 52-65. https://doi.org/10.37934/cfdl.14.12.5265

[16] Ariffin, Noor Amalina Nisa, Iskandar Waini, Abdul Rahman Mohd Kasim, Mohamad Hidayad Ahmad Kamal, Mohd Rijal Ilias, and Seripah Awang Kechil. "Flow and heat transfer analysis on reiner-philippoff fluid flow over a stretching sheet in the presence of first and second order velocity slip and temperature jump effects." *CFD Letters* 15, no. 1 (2023): 88-102. https://doi.org/10.37934/cfdl.15.1.88102

[17] Fábregas, Jonathan, Henry Santamaria, Edgardo Buelvas, Saul Perez, Carlos Díaz, Javier Andrés Carpintero Durango, Ricardo Mendoza, and Jennifer Villa. "Computational fluid dynamicsmodeling of microchannels cooling for electronic microdevices." *IIUM Engineering Journal* 23, no. 1 (2022): 384-396. https://doi.org/10.31436/iiumej.v23i1.2113

[18] Carpintero, Javier, Fausto A. Canales, Jonathan Fábregas, and José Ávila. "Factors and interactions that influence the pressure drop across an air volume reducing device on low-pressure water distribution networks." *Iranian Journal of Science and Technology, Transactions of Civil Engineering* 46, no. 2 (2022): 1433-1443. https://doi.org/10.1007/s40996-021-00682-z

[19] Sun, Zhijun, Jian Chen, Li Hou, Ma Dengqiu, and Haiyan Zhang. "Sliding friction contact stiffness model of involute arc cylindrical gear based on fractal theory." *International Journal of Engineering* 30, no. 1 (2017): 109-119. https://doi.org/10.5829/idosi.ije.2017.30.01a.14

[20] Carpintero, Javier, Brayan Martinez, Jonathan Fábregas, José Pérez, and Fausto A. Canales. "Hydraulic Characterization of a Check Valve for Low-Pressure Potable Water Distribution Applications." *Water* 15, no. 13 (2023): 2475. https://doi.org/10.3390/w15132475

[21] Tey, Wah Yen, and Hooi Siang Kang. "Power Loss in Straight Polygon Pipe via CFD Simulation." *Progress in Energy and Environment* (2018): 1-10.

[22] Tey, Wah Yen, Yutaka Asako, Nor Azwadi Che Sidik, and Rui Zher Goh. "Governing equations in computational fluid dynamics: Derivations and a recent review." *Progress in Energy and Environment* (2017): 1-19.

[23] Heng, Yap Jun, Nurul Farhana Mohd Yusof, Lee Ann Yen, Shazlina Abd Hamid, and Nurul Nadzirah Mohd Yusof. "A Contact Characteristic of Roller Bearing with Palm Oil-based Grease Lubrication." *Journal of Advanced Research in Fluid Mechanics and Thermal Sciences* 89, no. 2 (2022): 139-149. https://doi.org/10.37934/arfmts.89.2.139149.

[24] How, Heoy Geok, Yeoh Jun Jie Jason, Yew Heng Teoh, and Hun Guan Chuah. "Investigation of tribological properties of graphene nanoplatelets in synthetic oil." *Journal of Advanced Research in Fluid Mechanics and Thermal Sciences* 96, no. 1 (2022): 115-126. https://doi.org/10.37934/arfmts.96.1.115126

[25] Shlash, Bassam Amer Abdulameer, and Ibrahim Koç. "Turbulent fluid flow and heat transfer enhancement using novel Vortex Generator." *Journal of Advanced Research in Fluid Mechanics and Thermal Sciences* 96, no. 1 (2022): 36-52. https://doi.org/10.37934/arfmts.96.1.3652

[26] Rasep, Zuraidah, Muhammad Noor Afiq Witri Muhammad Yazid, Syahrullail Samion, and Nor Azwadi Che Sidik. "Potential of RBD Palm Oil as a Lubricant in Textured Journal Bearing using CFD with Consideration of Cavitation and Conjugate Heat Transfer." *CFD Letters* 14, no. 2 (2022): 98-110. https://doi.org/10.37934/cfdl.14.2.98110

[27] Larsson, Roland. "Transient non-Newtonian elastohydrodynamic lubrication analysis of an involute spur gear." *Wear* 207, no. 1-2 (1997): 67-73. https://doi.org/10.1016/S0043-1648(96)07484-4

[28] Zhao, Jing-jing, You-qiang Wang, Ping Zhang, and Guang-xiao Jian. "A Newtonian thermal elastohydrodynamic lubrication model for ferrofluid-lubricated involute spur gear pair." *Lubrication Science* 32, no. 2 (2020): 33-45. https://doi.org/10.1002/ls.1483

[29] Rezaei, E., M. Poursina, and M. Rezaei. "Experimental Investigation of Spur Gear Tooth Crack Location and Depth Detection using Short-time Averaging Method and Statistical Indicators." *International Journal of Engineering* 33, no. 10 (2020): 2079-2086. https://doi.org/10.5829/IJE.2020.33.10A.26